



Cu(II) complexes of 2-indole thiocarbohydrazones: synthesis, characterization and DNA cleavage studies

SHRIDHAR PAWAR^a, ANITA AMATE^a, DEBAMITRA CHAKRAVARTY^a,
RAYMOND J BUTCHER^b and ANUPA A KUMBHAR^{a,*}

^aDepartment of Chemistry, Savitribai Phule Pune University, Pune 411007, India

^bDepartment of Chemistry, Howard University, 2400 Sixth Street NW, Washington, DC 20059, USA

E-mail: anupa.kumbhar@unipune.ac.in

MS received 3 March 2021; revised 1 July 2021; accepted 5 July 2021

Abstract. Two Schiff base ligands FT1 and FT2 and their Cu(II) complexes were synthesized and characterized by ¹H NMR, ESI-MS, IR, UV-Visible, Fluorescence spectroscopy, EPR and single-crystal X-ray diffraction studies. FT1 crystallizes in the triclinic system while FT2 in the orthorhombic. The DNA cleavage activity of Cu(II) complexes was studied using plasmid pBR322 DNA by gel electrophoresis. All compounds cleave DNA on photoirradiation by oxidative mechanism.

Keywords. Thiocarbohydrazone; copper(II) complexes; fluorescence; crystal structure; DNA cleavage.

1. Introduction

Biologically active transition metal complexes contribute to an increasing research area for drug development. Indole is an aromatic heterocycle in which a benzene ring is fused to a five-membered pyrrole ring.¹ It is one of the important constituents of perfume and precursor of many pharmaceuticals. Indole derivatives are important dyestuff.² Indole containing natural and synthetic products such as indolemycin, mitomycin, pindolol, reserpine, are being used for the treatment of various illnesses. Many compounds containing indole nucleus have been reported to possess a wide variety of biological properties such as anti-inflammatory,^{3,4} cardiovascular,⁵ antibacterial,⁶ antiviral⁷ and cyclooxygenase-2 inhibitory activity.⁸

Thiocarbohydrazide derivatives^{9,10} have attracted much attention in recent years due to their application in the synthesis of heterocyclic compounds,¹¹ synthesis of transition metal complexes¹² and their pharmacological studies.¹³ This class of N, S donor ligands with variable donor

abilities yielded structurally diverse mono-, di-, tri- and polynuclear complexes mainly because thiocarbohydrazones can coordinate in either anionic or neutral form.¹⁴

Copper is a bio-essential element that plays a major role in electron transfer, oxygen transport, energy metabolism, mitochondrial respiration, anti-oxidation, collagen cross-linking, and pigmentation. Copper has high Lewis acidity which eventually facilitates DNA cleavage. Being the primary target for the development of new therapeutic agents, the interaction of small molecules with DNA is of paramount importance.^{15–19} Investigating the nuclease activity of small molecules help in elucidating their mechanism of action.²⁰

Thus, this manuscript focuses on the synthesis of two new 3-formyl indole thiocarbohydrazone ligands and their Cu(II) complexes. The compounds are characterized by IR, NMR, UV-Visible, fluorescence, EPR and mass spectroscopy. Single-crystal x-ray structures of both the ligands are also reported. The potential of these compounds as DNA cleaving agents is reported.

*For correspondence

2. Experimental

2.1 Chemicals

All chemicals used in this work were of analytical reagent grade. The chemicals and sources were as follows: indole, thiocarbohydrazide (TCH), sodium hydroxide, $\text{CuCl}_2 \cdot 2\text{H}_2\text{O}$, DMSO, acetone, ethanol, acetonitrile, DMF, ether were obtained from S. D. Fine Chemicals Limited and used as received. Supercoiled plasmid *pBR322* DNA was purchased from SRL (India). Deionized water was used for the preparation of buffer solutions.

2.2 Measurements

UV-Visible absorption spectra were recorded on a JASCO FP-8300 and Shimadzu UV-1800 spectrophotometer available at the Department of Chemistry, S. P. Pune University. Fluorescence measurements were carried out on the Shimadzu RF5301 spectrometer. All measurements were performed using a 3 cm \times 3 cm quartz cuvette. The infrared spectra of solid samples dispersed in KBr pellets were recorded on a BRUKER Platinum ATR Tensor-37 spectrophotometer. ^1H and ^{13}C NMR spectra were recorded on a Varian-Mercury 300 MHz spectrometer with DMSO-d_6 as solvent at 25°C and all chemical shifts are given relative to tetramethylsilane (TMS) as the internal standard. Electrospray ionization mass spectral measurements were performed on Bruker Nano-Advance UHPLC LC-MS-MS with TOF analyzer at Central Instrumentation Facility of S. P. Pune University. X-band EPR spectra were recorded as powder and DMF glass on ESR-JEOL model JES-FA200 spectrometer at liquid nitrogen temperature at the Indian Institute of Technology Bombay, Mumbai, India. Magnetic susceptibility measurements were performed at 28°C on Magnetic Susceptibility Balance from Sherwood Scientific, Cambridge, UK at Pratap College, Amalner.

2.3 X-ray data collection and refinement

Single crystals of the FT1 and FT2 were grown by slow evaporation of their solution in acetonitrile and acetone respectively. Data was collected on D8 Venture PHOTON 100 CMOS diffractometer using Mo- K_α radiation ($\lambda = 0.071 \text{ \AA}$), with exposure/frame = 15 secs. The X-ray generator was operated at 50 kV and 1 mA. An initial set of cell constants and an orientation matrix were calculated from total of 24

and 60 frames for Mo- K_α . The optimized strategy used for data collection consisted of different sets of φ and ω scans with 0.5° steps in φ/ω . Crystal to detector distance was 5.00 cm. Data integration was carried out by the Bruker SAINT program and empirical absorption correction for intensity data were carried out by Bruker SADABS. The Programs are integrated into APEX II package.²¹ The data were corrected for Lorentz and polarization effect. The structures were solved by the direct method using SHELX-97.²² The final refinement of the structures was performed by full-matrix least-squares technique with anisotropic thermal data for non-hydrogen atoms on F^2 . The hydrogen atoms were refined at calculated positions as riding atoms with isotropic displacement parameters. Molecular diagrams were generated using ORTEP-3²³ and Mercury programs.²⁴ Geometrical calculations were performed using SHELXTL²² and PLATON.²⁵ The crystal data of FT1 and FT2 in the cif format has been deposited in the Cambridge Crystallographic Data Centre with CCDC numbers 2007996 and 2007997 respectively. This data can be obtained free of charge via <http://www.ccdc.cam.ac.uk/conts/retrieving.html>, or from the Cambridge Crystallographic Data Centre, 12 Union Road, Cambridge CB2 1EZ, UK; fax: (+44) 1223-336-033; or email: deposit@ccdc.cam.ac.

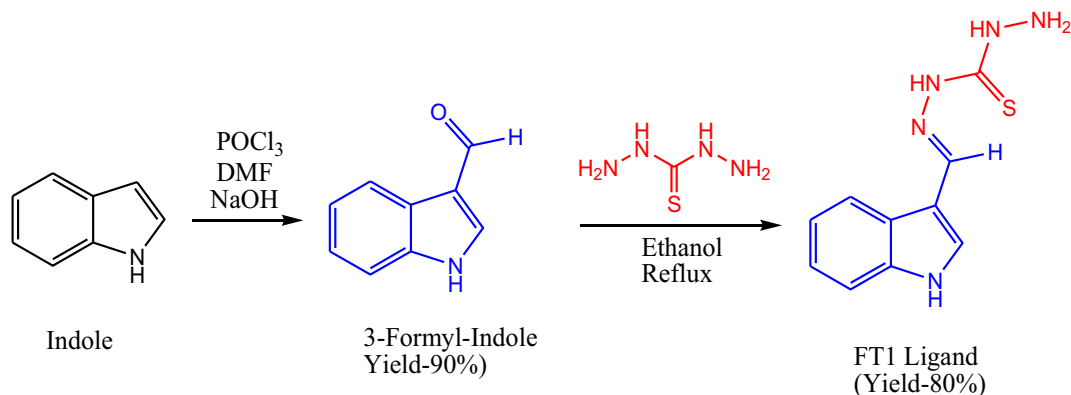
2.4 DNA cleavage studies

The cleavage of *pBR322* DNA was determined by 1% agarose gel electrophoresis. The DNA cleavage ability of ligands and complexes was studied in Tris-Boric acid-EDTA (TBE) buffer. Supercoiled *pBR 322* plasmid DNA was treated with Cu(II) complexes (20, 40, 60 and 80 M) and the mixture was (total volume 10 μL) incubated for 30 min in dark at 37°C followed by irradiation at 364 nm for 40 min. Then 2 μL of blue juice (bromophenol blue, xylene cyanol in 40% glycerol and 0.2 M EDTA) was added to quench the reaction. Sample solutions were loaded onto 1% agarose gel and run at a constant voltage of 60 V for 3-4 h in the buffer solution. The gel was stained with 0.5 g/mL ethidium bromide, de-stained in distilled water for 15 min and visualized under UV light. Photographs were taken using Alpha Innotech gel documentation system (AlphaImager 2200). To know the mechanism of DNA cleavage by these complexes, another experiment was carried out by adding scavenging agents such as DMSO, mannitol, DABCO, L-histidine, sodium azide, and superoxide dismutase (SOD) prior to the addition of complexes. The

concentrations of scavenging agents given in parentheses in the caption of figures correspond to the stock concentration.

Synthesis of 3-formylindole thiocarbohydrazone, FT1

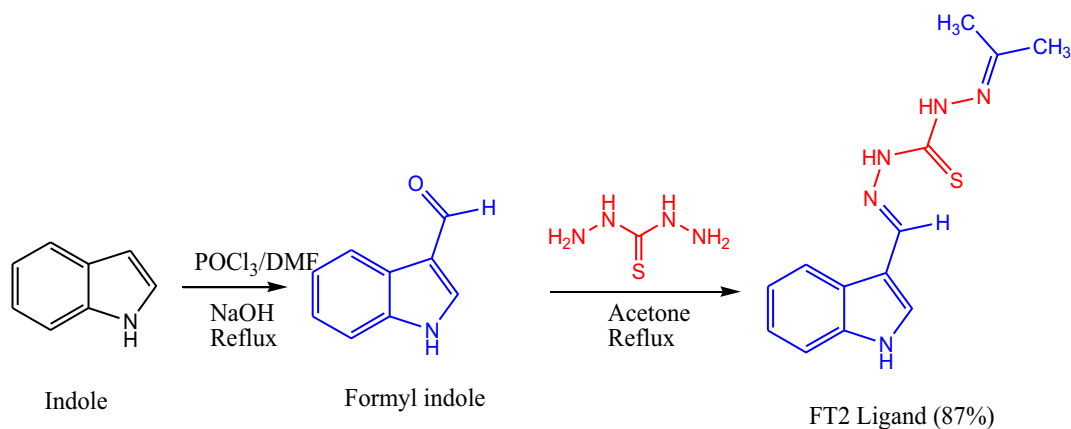
6.8 mmol) in ethanol, and the reaction mixture was refluxed for 3 h in presence of catalytic amount of acetic acid. Progress of reaction was monitored by TLC (pre-coated silica gel plate; 3:7 (v/v) ethyl acetate:hexane). The resulting light-yellow solid was filtered washed



3-formyl indole was synthesized by the reported procedure.²⁶ Solutions of indole (0.5 g, 4.27 mmol) and POCl₃ (0.655 g, 4.27 mmol) in DMF (0.312 g, 4.27 mmol) were mixed at 0°C with vigorous stirring. After bringing the solution to room temperature, the reaction was refluxed for 1 h. The pH of the reaction mixture at this juncture was 5.0, which was adjusted between 8 and 9 with ~ 20 mL 1 M NaOH and refluxing was continued for another hour. Reaction progress was monitored by TLC. In the end, the reaction mixture was poured into ice-cold water. The white precipitate obtained was filtered, washed with water and dried in a vacuum. Yield = 90%; ESI-MS (*m/z*): M = C₉H₇NO = 145.05; found [M+H]⁺ 146.06 (Figure S19, SI).

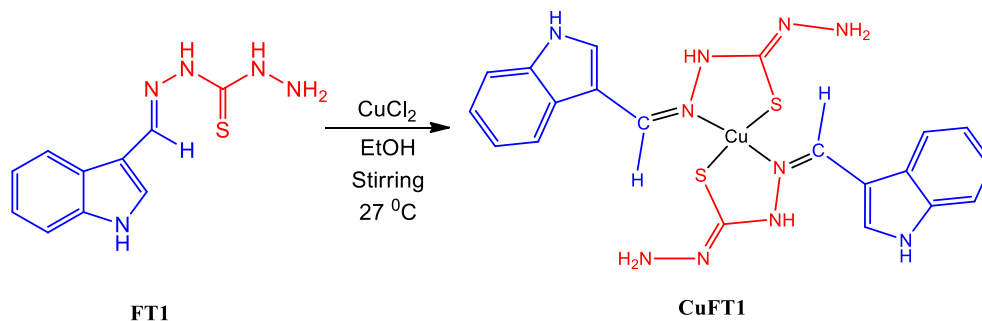
Thiocarbohydrazone, TCH, (0.073 g, 6.8 mmol) was added to the solution of 3-formyl indole (0.100 g,

with distilled water and recrystallized from ethylacetate to obtain a crystalline compound. Yield 86%; ¹H-NMR (500 MHz, DMSO d₆, δ ppm): 1.3 (m, 1H, NH), 2.1(d, 2H, NH₂), 7.2(s, 1H, NH), 7.3(dd, 1H aromatic protons), 7.4 (dd, 1H aromatic proton), 7.6(d, 1H, aromatic proton), 7.8(s, 1H, aromatic proton), 8.3(d, 1H, aromatic proton), 9.1 (s, 1H, =C-H), 10.2 (s, 1H, aromatic -NH); ¹³C-NMR (DMSO d₆): δ = 111.0 (Ar-C1), 112.1 (Ar-C2), 121.0 (Ar-C3), 122.6(Ar-C4), 123.1 (Ar-C5), 124.5 (Ar-C6), 131.2 (Ar-C7), 137.4 (Ar-C8), 141.3 (C9=N), 173.4 (C10=S); IR ν, cm⁻¹: 3310 (N-H), 1510 (C=N), 1112 (C=S). UV-Visible (DMSO) λ_{max} (nm) = 280, 332; Fluorescence (DMSO, λ_{ex} = 332 nm): 395 nm; ESI-MS (*m/z*): [M+H]⁺ 234.08.



2.5 Synthesis of acetone 3-formyl indole thiocarbohydrazone, FT2

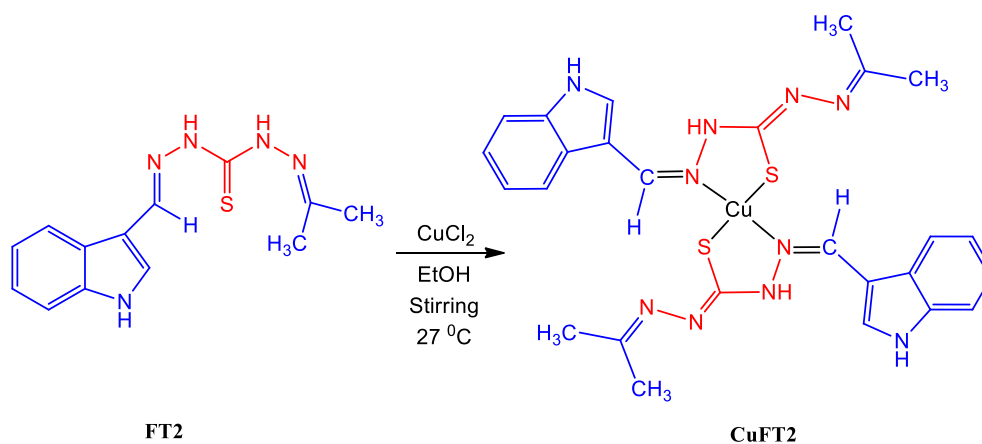
2.6 Synthesis of Cu(II) complex of FT1; (CuFT1)



This ligand was synthesized by same procedure to that of FT1 using acetone as a solvent. The resulting yellow solid was filtered, washed with distilled water and recrystallized from acetone to obtain a crystalline compound. Purity of the product was checked on TLC (precoated silica gel plate; 3:7 (v/v) ethyl acetate:hexane). Yield 90%; $^1\text{H-NMR}$ (500 MHz, DMSO d_6 , δ ppm): 2.1 (s, 6H, CH_3), 7.25 (s, 1H, -NH), 7.3 (s, 1H, -NH), 7.4 (m, 1H, aromatic proton), 7.7 (m, 1H, aromatic proton), 8.1 (d, 1H, aromatic proton), 8.3 (s, 1H, aromatic proton), 8.6 (d, 1H, aromatic proton), 10.1 (s, 1H, =C-H), 11.5 (s, 1H, aromatic -NH); $^{13}\text{C-NMR}$ (DMSO d_6): δ =21.0 (C-C1), 30.0 (C-C2), 79.0 (Ar-C3), 80.0 (Ar-C4), 111.0 (Ar-

FT1 and $\text{CuCl}_2 \cdot 2\text{H}_2\text{O}$ were dissolved in EtOH separately and mixed with vigorous stirring. The reaction was stirred for 3 h at room temperature. Progress of the reaction was monitored by TLC (alumina precoated plates; 1:9 (v/v) methanol:chloroform). The resulting brown coloured solid was filtered, washed with diethylether and dried under vacuum (Yield: 80%). IR ν, cm^{-1} : 3350 (N-H), 1610 (C=C), 1560 (C=N), 1150 (C=S). UV-Visible (DMSO) λ_{max} (nm) = 270, 410. Fluorescence (DMSO, λ_{ex} = 332 nm): 448 nm; ESI-MS (m/z): $[\text{M}+\text{H}]^+$ 528.06.

2.7 Synthesis of $[\text{Cu}(\text{FT}_2)_2]$ complex (CuFT2)



C5), 112.0 (Ar-C6), 120.0 (Ar-C7), 123.0 (Ar-C8), 124.0 (Ar-C9), 131.0 (Ar-C10), 137.0 (C11=N), 174.0 (C12=N), 176.0 (C13=S); IR ν, cm^{-1} : 3312 (N-H), 1500 (C=N), 1200 (C=S). UV-Visible (DMSO) λ_{max} (nm) = 280, 340; Fluorescence (DMSO, λ_{ex} = 340 nm): 385 nm; ESI-MS (m/z): $[\text{M}+\text{H}]^+$ 274.11.

Same procedure to that of CuFT1 was used to synthesize this complex. The resulting brown coloured solid was filtered, washed with diethylether and dried.

Purity of the product was checked on TLC (alumina pre-coated plates; 1:9 (v/v) methanol:chloroform) (Yield: 85%). IR ν, cm^{-1} : 3300 (N-H), 1610 (C=C), 1460 (C=N), 1100 (C=S); UV-Visible (DMSO) λ_{max} (nm) = 270, 345, 560; Fluorescence (DMSO, λ_{ex} = 345 nm): λ_{em} = 410 nm; ESI-MS (m/z): $[\text{M}+\text{H}]^+$ 609.13.

3. Results and Discussion

3.1 Synthesis and characterization

The copper(II) complexes were prepared by direct reaction of ligands with copper(II) chloride in acetone in 2:1 molar ratio. The compounds were characterized by IR, UV-Vis, fluorescence and mass spectroscopy. The ^1H NMR spectrum of FT1 recorded in DMSO- d_6 solvent (Figure S1, SI) shows peak at 10.2 ppm which is assigned to N-H proton of indole. A singlet at 9.1 is assigned to N=CH connecting to thiocarbohydrazide side chain while peaks in the range 7.2 to 8.3 are assigned to aromatic protons. Ligand FT2 (Figure S4, SI) shows a peak at 2.1 ppm corresponding to six methylenic protons. Indole's NH appear at 11.5 ppm, aromatic protons appear in the range 7.2 to 8.6 ppm while N=CH connecting to thiocarbohydrazide side-chain appear at 10.1 ppm. ^{13}C -NMR spectra of FT1 and FT2 were recorded in DMSO d_6 (Figures S3 and S5, SI). Both the ligands show resonances due to thiocarbonyl (C=S) at 173.38 and 176.0 ppm, respectively. The imine carbon (C=N) in FT1 gives signal at 120.28 whereas for FT2 it appears at 137.0 ppm. Another signal at 174 ppm in FT2 is attributed to terminal (C=N) formed after conjugation with acetone. The resonances of aryl carbons appear in the region 111-137.4 ppm. Chemical shifts for all other carbons were observed in the expected region and the data is given in Section 2.

The mass spectra of the ligands and their complexes are shown in Figures S7-S10, SI. FT1 shows peaks at m/z = 234.08 and 256.06 which correspond to $[\text{M} + \text{H}]^+$ and $[\text{M} + \text{Na}]^+$ respectively whereas peaks at m/z = 217.05 and 279.11 are due to $[\text{M}-\text{NH}_2+\text{H}]^+$ and $[\text{M}+\text{H}+\text{CH}_3\text{CN}]^+$ respectively. CuFT1 complex shows a molecular ion peak at m/z = 528.06 corresponding to $[\text{M}+\text{H}]^+$ and m/z = 569.10 to $[\text{M} + \text{CH}_3\text{CN}]^+$. Similarly, in ligand FT2, a peak at m/z = 274.11 corresponds to $[\text{M}+\text{H}]^+$ and m/z = 296.11 to $[\text{M}+\text{Na}]^+$. CuFT2 gives a molecular ion peak, which is also a base peak, at m/z = 609.13 corresponding to $[\text{M}+\text{H}]^+$.

FT1 and FT2 show thione-thiol tautomerization as both the ligands contain a proton adjacent to thione

group (C=S). IR spectrum of FT1 shows symmetric and asymmetric stretches of NH_2 at 3100 and 3310, $\nu(\text{N-H})$ at 3180 cm^{-1} , respectively and a sharp peak at 3375 which is assigned to intramolecular hydrogen bonding in ligand. The presence of $\nu(\text{N-H})$ stretch at 3180 cm^{-1} , and the absence of $\nu(\text{S-H})$ in the region $2500\text{-}2600 \text{ cm}^{-1}$ suggests that both the ligands are in thione form in the solid state. The C=N and C=S frequencies appear at 1510 and 1112 cm^{-1} , respectively. In CuFT1 symmetric and asymmetric stretches of NH_2 appear at the same position indicating that the terminal amine group is not involved in metal complexation. In CuFT1, C=N and C-S frequencies are shifted and appear at 1560 and 1150 cm^{-1} , respectively, indicating the involvement of nitrogen and sulphur in metal coordination. The absence of symmetric and asymmetric stretches of NH_2 in the ligand FT2 confirms substitution of terminal NH_2 by $\text{C}(\text{CH}_3)_2$ group. Here, $\nu(\text{N-H})$ appears at 3180 cm^{-1} and a sharp peak at 3312 cm^{-1} is assigned to intramolecular hydrogen bonding. $\nu(\text{C=N})$ appears at 1500 cm^{-1} while $\nu(\text{C=S})$ appears at 1200 cm^{-1} . In the corresponding Cu(II) complex, $\nu(\text{N-H})$ appears at 3150 cm^{-1} and peak intramolecular hydrogen bonding is observed at 3330 cm^{-1} . The shift in $\nu(\text{C=N})$ and $\nu(\text{C=S})$ to 1460 and 1100 cm^{-1} respectively in the CuFT2 complex indicates involvement of sulphur and azomethinic nitrogen in copper coordination (Figures S11-S14, SI).

Absorption spectra of FT1, FT2, CuFT1 and CuFT2 ($10 \mu\text{M}$) were recorded in DMSO solvent (Figure 1). The absorption spectra of FT1 and FT2 are dominated by the intraligand $n \rightarrow \pi^*$ and $\pi \rightarrow \pi^*$ transitions. Their corresponding Cu(II) complexes show ligand-to-metal charge transfer bands at 410 nm (CuFT1) and 560 nm (CuFT2), respectively along with the ligand-based transitions.

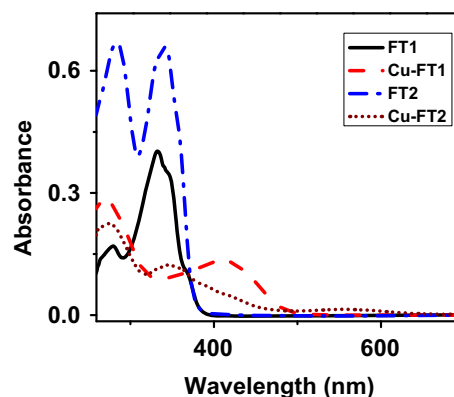


Figure 1. Absorption spectra of $10 \mu\text{M}$ solutions of FT1 (black solid), CuFT1 (red dash), FT2 (blue dash dot) and CuFT2 (brown short dot) in DMSO solvent.

The fluorescence spectra of the ligands and complexes are shown in Figure 2. FT1, when excited at 332 nm, gave a broad peak centered at 395 nm

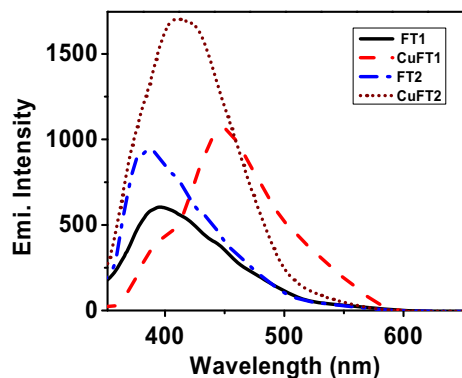


Figure 2. Fluorescence spectra of 10 μM solutions of FT1 (black solid), CuFT1 (red dash), FT2 (blue dash dot) and CuFT2 (brown short dot) in DMSO solvent. The complexes were excited at the same wavelengths to that of their respective ligands.

whereas FT2 when excited at 340 nm gave an emission peak at 385 nm. Typically, the emission intensity of a fluorescent ligand is quenched on complexation with a paramagnetic metal ion like Cu(II). However, enhanced fluorescence intensity upon complexation suggests a coordination-related phenomenon. This can be attributed to the separation of excited states of Cu(II) and the ligand through distortion in the geometry of CuFT1 and CuFT2 in the excited state.^{27,28} Investigations carried out by Holland and coworkers employing the single photon emission experiments combined with the density functional theoretic calculations on pyrene functionalized bis(thiosemicarbazonato) copper(II) complexes led to similar inferences.²⁹

Single crystals of FT1 and FT2 suitable for X-ray diffraction were obtained by slow evaporation of acetonitrile and acetone solutions, respectively. An ORTEP representation of FT1 and FT2 along with their atom numbering scheme is shown in Figures 3

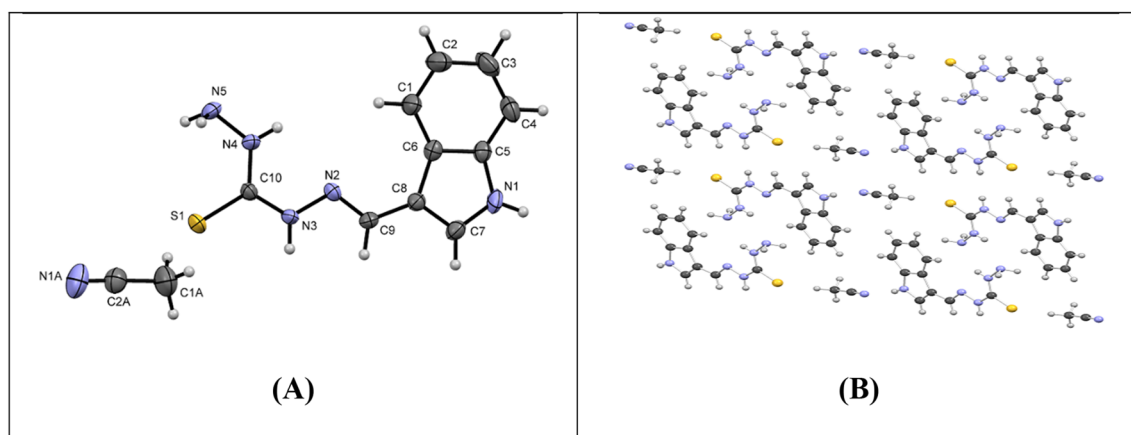


Figure 3. (A) ORTEP showing 50% thermal ellipsoids and atom numbering for FT1; (B) packing down a axis.

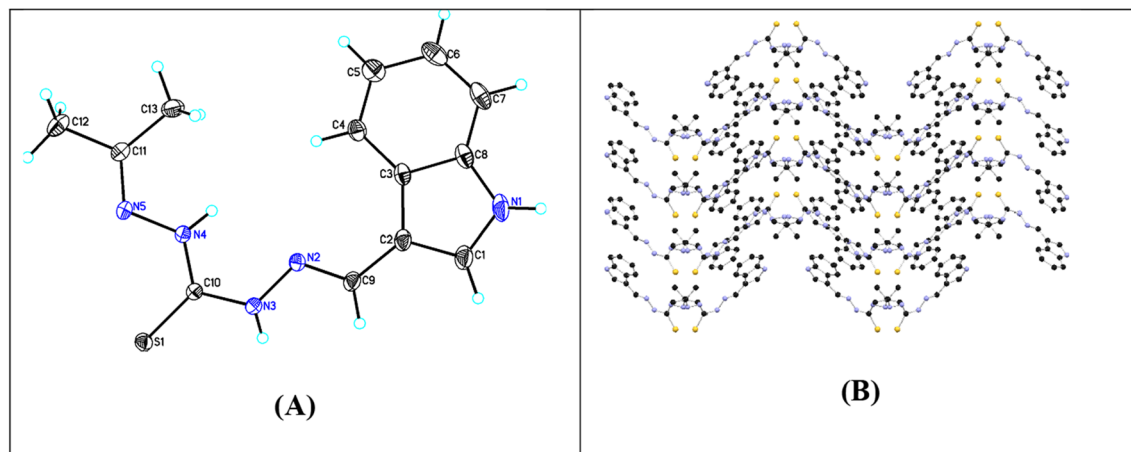


Figure 4. (A) ORTEP showing 50% thermal ellipsoids and atom numbering for FT2; (B) packing down a axis.

Table 1. Crystallographic parameters for FT1 and FT2.

	FT1	FT2
Empirical formula	C ₂₄ H ₃₀ N ₁₀ O ₂ S ₂	C ₁₃ H ₁₅ N ₅ S
Formula weight	554.70	273.36
Temperature	293 K	273 K
Wavelength	1.54178 Å	0.71073 Å
Crystal system	Triclinic	Orthorhombic
Space group	P-1	P b c a
Unit cell dimensions	a = 5.2903(12) Å b = 14.773(3) Å c = 17.783(4) Å α = 99.6(9)° β = 91.505(10)° γ = 96.147(10)°	a = 14.0462(10) Å b = 10.5925(7) Å c = 18.7154(12) Å α = 90° β = 90° γ = 90°
Volume	1360.7(5) Å ³	2784.6(3) Å ³
Z	2	8
S	1.058	1.099
Density(calculated)	1.354 mg/m ³	1.304 mg/m ³
Absorption coefficient	2.124 mm ⁻¹	0.226 mm ⁻¹
F(000)	584	1152.0
Crystal size	0.490 × 0.100 × 0.080 mm ³	0.30 × 0.26 × 0.12 mm ³
Theta range for data	3.054 to 68.506°	2.900 to 28.610°.
Collection		
Index ranges	-6 ≤ h ≤ 6, -17 ≤ k ≤ 17, -21 ≤ l ≤ 21	-18 ≤ h ≤ 18, -13 ≤ k ≤ 14, -25 ≤ l ≤ 25
Reflections collected	11492	34829
Independent reflections	4597 [R(int)=0.0889]	3533 [R(int) = 0.1101]
Completeness to theta =67.679°	91.7%	99.9%
Refinement method	Full matrix least squares on F ²	Full-matrix least-squares on F ²
Data/restraints/parameters	4597/0/345	3533/0/174
Goodness-of-fit on F ²	1.257	1.067
R(reflections)	0.0998(2853)	0.0612(2072)
wR2(reflections)	0.3115(4565)	0.1231(3533)
Largest diff. peak and hole	0.737 and -0.594 e.Å ⁻³	0.439 and -0.307 e.Å ⁻³

and 4, respectively. A summary of the crystallographic data is compiled in Table 1, selected bond lengths and bond angles are given in Table S1, SI. The compound FT-1 crystallizes in the triclinic space group P-1 with one molecule of acetonitrile solvent in the asymmetric unit having two molecules. Two molecules FT1 form a dimer *via* intermolecular N3–H...S hydrogen-bonding interactions (Figure S15, SI). This molecule also interacts with a solvent molecule *via* N1–H...O2 hydrogen-bonding thus growing into an infinite chain. It does not show π–π and C–H—π interactions. Single crystals of compound FT-2 crystallizes in the orthorhombic space group P_{bca} with the asymmetric unit. There exist weak C–H—π interactions (C1–C6—H3, C4–C5—H9, S1–C10—H13), intermolecular hydrogen-bonding in FT2 (Figure S16, SI) and no π–π interaction.

With N₂S₂ coordination, the formation of dimeric copper(II) complexes cannot be ruled out. To ascertain that, the NMR spectra of CuFT1 and CuFT2 were

recorded in DMSO-d₆ which are very broad and show the merging of the ligand peaks indicating the paramagnetic nature of the copper centre (Figure S2 and S5, SI respectively).

The stabilization of copper in the +2 oxidation state was confirmed by X-band EPR spectra. The EPR spectra were recorded as powder samples as well as in DMF (Figure 5) at liquid nitrogen temperature. The powder EPR spectra of both the complexes are axial and do not show any signal at half-field (Figure S20, SI) indicating the absence of dimer. The structural similarity of the complexes is reflected in their EPR, which are quite comparable with minor differences in their g values (Table 2). The splitting of the g_{||} signals is noticed only in DMF and does not correspond to the hyperfine splitting. Considering the coordinating nature of DMF and square planar geometry of the complexes, the formation of a new DMF coordinated species in solution cannot be ruled out; which may be responsible for this splitting. The g_{||} values for CuFT1

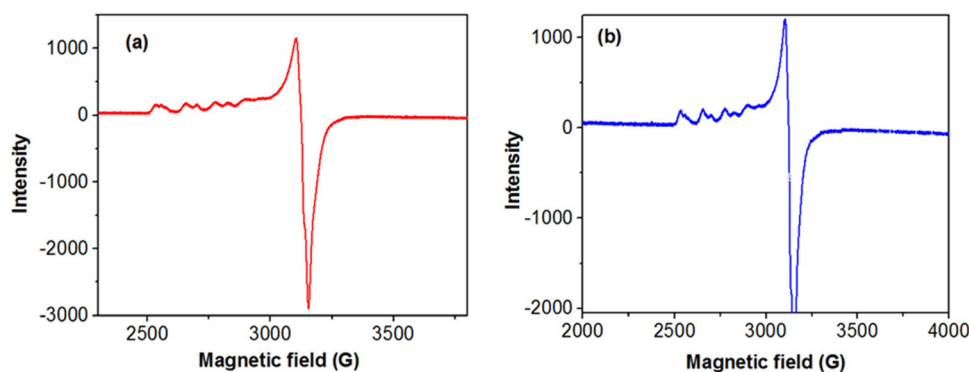


Figure 5. X-band EPR spectra of (a) CuFT1 and (b) CuFT2 recorded in DMF at liquid nitrogen temperature.

Table 2. EPR parameters for CuFT1 and CuFT2 for powder samples and in DMF recorded at liquid nitrogen temperature

Complex	g_{\parallel}	g_{\perp}	$A_{\text{II Cu}} \text{ G}$
CuFT1	2.110 (powder)	2.040 (powder)	–
	2.364 (DMF)	2.086 (DMF)	182.7
CuFT2	–	2.160 (powder)	–
	2.363 (DMF)	2.080 (DMF)	185.2

and CuFT2 in DMF are 2.364 and 2.363 and g_{\perp} values are 2.086 and 2.080, respectively. The hyperfine coupling constant for copper listed in Table 2 is similar to other N_2S_2 donor systems reported in the literature.^{30,31} As $g_{\parallel} > g_{\perp} > 2$, the complexes adapt square planar geometry with unpaired electron residing in $d_{x^2-y^2}$ orbital.

The magnetic moment of CuFT1 and CuFT2 recorded at 28°C were found to be 1.89 and 1.83 B.M. respectively which are slightly higher than the spin only magnetic moment value of 1.73 for Cu(II).

3.2 DNA cleavage studies

It is known that DNA cleavage depends on the relaxation of supercoiled circular conformation of plasmid pBR322 DNA to nicked circular or linear conformations. The fastest migration will be observed for DNA of closed circular conformations (form II) when potential is applied to circular plasmid DNA. The supercoil relaxes to form a slower-moving nicked conformation (form II) if one of the strands is cleaved. The cleavage of both strands leads to a linear conformation (form III) which migrates between supercoiled and the nicked circular forms.^{32,33}

The DNA cleavage experiments were performed using 1% agarose gel electrophoresis. Both the complexes do not show DNA cleavage when incubated in dark at 37°C for 30 min (Figures S15 and S16, SI). The compounds were then irradiated under monochromatic UV light (364 nm) for 40 min wherein concentration-dependent cleavage of DNA was observed in the complexes (Figure 6).

Further, experiments were carried out in presence of radical scavengers such as DMSO ($\bullet\text{OH}$), mannitol ($\bullet\text{OH}$), DABCO ($^1\text{O}_2$), L-Histidine ($^1\text{O}_2$), NaN_3 ($^1\text{O}_2$), and superoxide dismutase (SOD, $\text{O}_2^{\bullet-}$) to investigate the mechanism of DNA cleavage upon photoirradiation.

DNA cleavage by CuFT1 was inhibited in presence of DMSO (Figure 7, lane 2), L-Histidine (Figure 7, lane 5) and sodium azide (Figure 7, lane 6) suggesting that hydroxyl radicals and to some extent singlet oxygen are involved in DNA cleavage.

CuFT2 was found to be inhibited to some extent by DMSO (Figure 8, lane 3) suggesting the involvement of hydroxyl radicals in the DNA cleavage.

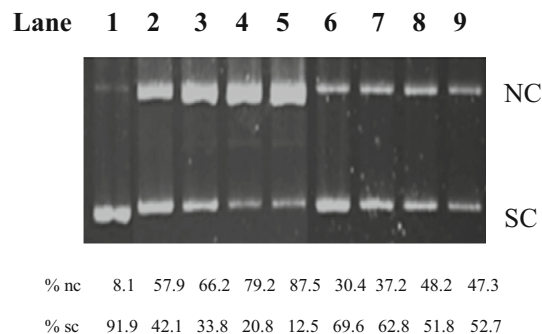


Figure 6. Photograph of 1% agarose gel of plasmid pBR322 DNA when incubated at 37°C for 30 min with CuFT1 and CuFT2 followed by irradiation for 40 min. [DNA] = 100 ng, Lane 1 = DNA control, Lanes 2-5, DNA + CuFT1 (20, 40, 60, 80 μM); Lanes 6-9, DNA + CuFT2 (20, 40, 60, 80 μM).

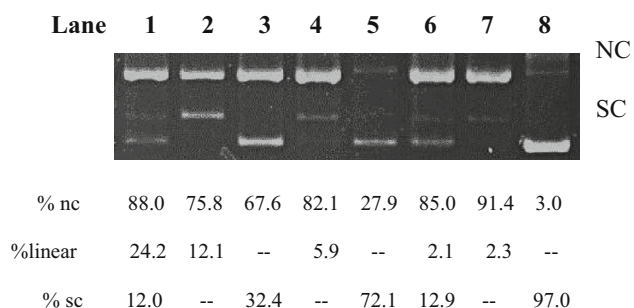


Figure 7. Photograph of 1% agarose gel showing the effect of inhibitors on cleavage of pBR322 DNA by CuFT1, [DNA] = 100 ng, [CuFT1] = 80 μ M. Lane 8 = DNA control; 1 = DNA + CuFT1; Lane 2 = DNA + CuFT1 + DMSO; Lane 3 = DNA + CuFT1 + mannitol (50 mM); Lane 4 = DNA + CuFT1 + DABCO (10 mM); Lane 5 = DNA + CuFT1 + L-histidine (20 mM); Lane 6 = DNA + CuFT1 + NaN₃ (20 mM); Lane 7 = DNA + CuFT1 + SOD (15 units).

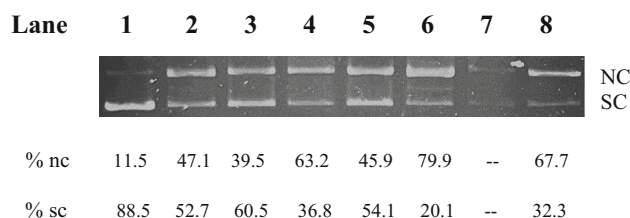


Figure 8. Photograph of 1% agarose gel showing the effect of inhibitors on cleavage of pBR322 DNA by CuFT2, [DNA] = 100 ng, [CuFT2] = 80 μ M. Lane 1 = DNA control; Lane 2 = DNA + CuFT2; Lane 3 = DNA + CuFT2 + DMSO; Lane 4 = DNA + CuFT2 + mannitol (50 mM); Lane 5 = DNA + CuFT2 + DABCO (10 mM); Lane 6 = DNA + CuFT2 + L-histidine (20 mM); Lane 7 = DNA + CuFT2 + NaN₃ (20 mM); Lane 8 = DNA + CuFT2 + SOD (15 units).

4. Conclusions

In summary, we have reported two thiocarbohydrazide ligands and their Cu(II) complexes. The complexes were monomeric and fluorescent. The Cu(II) complexes were able to cleave plasmid pBR322 DNA in a concentration-dependent manner on photoirradiation at 364 nm and the major species involved in DNA cleavage is hydroxyl radicals.

Supplementary Information (SI)

Figures S1-S21 and Table S1 are available at www.ias.ac.in/chemsci.

Acknowledgements

Financial support to SSP from Dr. Babasaheb Ambedkar National Research Fellowships (BANRF), Maharashtra, India, and Savitribai Phule Pune University (SPPU) is

gratefully acknowledged. The Central Instrumentation Facility (CIF) of Savitribai Phule Pune University is acknowledged for single-crystal X-ray structures and ESI HR-MS. We also acknowledge the Sophisticated Analytical Instrumentation Facility (SAIF) at the Indian Institute of Technology Bombay, Mumbai for EPR measurements. Kind assistance in magnetic susceptibility measurements by Prof. Jayesh Gujarathi, Pratap College, Amalner is gratefully acknowledged.

References

- Bose P and Ghosh P 2010 Visible and near-infrared sensing of fluoride by indole conjugated Urea/thiourea ligands *Chem. Commun.* **46** 2962
- Yadav B P, Ahmad I and Thakur M 2016 Synthesis of some novel indole derivatives as potential antibacterial, antifungal and antimalarial agents *IOSR J. Pharm.* **6** 27
- Kaushik N K, Kaushik N, Attri P, Kumar N, Kim C H, Verma A K and Choi E H 2013 Biomedical Importance of Indoles *Molecules* **18** 6620
- Tisato F, Marzano C, Porchia M, Pellai M and Santini C 2010 Copper in diseases and treatments, and copper-based anticancer strategies *Med. Res. Rev.* **30** 708
- Heque R A and Salam M A 2016 Synthesis, spectroscopic properties and biological activity of new mono organotin(IV) complexes with 5-bromo-2-hydroxybenzaldehyde-4,4-dimethylthiosemicarbazone *Cogent Chem.* **1** 282
- Rapheal P F, Manoj E and Kurup M R P 2007 Copper(II) complexes of N(4)-substituted thiosemicarbazones derived from pyridine-2-carbaldehyde: Crystal structure of a binuclear complex *Polyhedron* **26** 818
- Beckford F A, Shaloski J M, Leblanc G, Thessing J, Lewis-Alleyne L C, Holder A A, et al. 2009 Microwave synthesis of mixed ligand diimine-thiosemicarbazone complexes of ruthenium(II): biophysical reactivity and cytotoxicity *Dalton Trans.* **48** 10757
- Bhat M A, Al-Omar M A, Raish M, Ansari M A, Abuelizz H A, Bakheit A H and Naglah A M 2018 Indole Derivatives as Cyclooxygenase Inhibitors: Synthesis, Biological Evaluation and Docking Studies *Molecules* **23** 1250
- Cheng H, Ying D C, Jie F C, Jiang L Y and Jin M Q 2000 Self-Assembly, Spectroscopic and Electrochemical Studies of Nickel(II)-4,8-Diazaundecanediamide Complex *Dalton Trans.* **9** 1207
- El-Sawaf A K, Nassar A F and El-Samanody S 2014 Synthesis, magnetic, spectral and biological studies of copper(II) complexes of 4-Benzoyl-3-methyl-1-phenyl-2-pyrazolin-5-one N(4)-substituted thiosemi-carbazones *Sci. J. Chem.* **3** 17
- Sthisha M P, Shetti U N, Revankar V K and Pai K S R 2008 Some Novel Schiff Bases from Pyruvic Acid with Amines Containing N & S Donor Atoms: Synthesis, Spectral Studies and X-Ray Crystal Structures *Eur. J. Med. Chem.* **43** 2338

12. Chattopadhyay S K and Mak T W 2000 Study of Cu²⁺ mediated oxidation of thiosemicarbazide, thiocarbohydrazide and thiourea *Inorg. Chem. Commun.* **3** 111
13. Bacchi A, Bonini A and Carcelli M 1996 Chelating behaviour of methyl 2-pyridyl ketone carbonyl- and thiocarbonohydrates in copper(II) and zinc(II) complexes *Dalton Trans.* **35** 185
14. Zhang N, Tai Y, Li M, Ma P, Zhao J and Niu J 2014 Main group bismuth(III), gallium(III) and diorganotin(IV) complexes derived from bis(2-acetylpyrazine)thiocarbonohydrate: synthesis, crystal structures and biological evaluation *Dalton Trans.* **43** 5182
15. Chitrapriya N, Shin J H, Hwang I H, Kim Y, Kim C and Kim S K 2015 Synthesis, DNA binding profile and DNA cleavage pathway of divalent metal complexes *RSC Adv.* **5** 68067
16. Mathur N and Bargotyia S 2016 DNA – Binding and Cleavage Studies of Macrocyclic Metal Complexes Containing Heteroatomic Ligands *Chem. Sci. Trans.* **5** 117
17. Viqueira J, Duran M L, Jose A, Vazquez G, Castro J, P-Iglesias C, et al. 2018 Modulating the DNA cleavage ability of copper(II) Schiff bases through ternary complex formation *New J. Chem.* **42** 15170
18. Jawoor S S, Patil S A and Toragalmath S S 2018 Synthesis and characterization of heteroleptic Schiff base transition metal complexes: a study of anticancer, antimicrobial, DNA cleavage and anti-TB activity *J. Coord. Chem.* **71** 271
19. Hossain M S, Roy P K, Zakaria C M and Zahan M K E 2018 Selected Schiff base coordination complexes and their microbial application: A review *Int. J. Chem. Stud.* **6** 19
20. Jia S, Wang R, Wu K, Jiang H and Du Z 2019 Elucidation of the Mechanism of Action for Metal Based Anticancer Drugs by Mass Spectrometry-Based Quantitative Proteomics *Molecules* **24** 581
21. Sheldrick G M 2015 *SHELXT* – Integrated space-group and crystal-structure determination *Acta Cryst.* **71** 3
22. Clegg W 2003 Some guidelines for publishing *SHELXL*-generated CIF results in *Acta Cryst.* **59** 2
23. Farrugia L J 1997 *ORTEP-3* for Windows - a version of *ORTEP-III* with a Graphical User Interface (GUI) *J. Appl. Cryst.* **30** 565
24. Macrae C F, Edgington P R, McCabe P, Pidcock E, Shields G P, Taylor R, et al. 2006 Mercury: visualization and analysis of crystal structures *J. Appl. Cryst.* **39** 453
25. Spek A L 2003 Single-crystal structure validation with the program *PLATON* *J. Appl. Cryst.* **36** 7
26. Xiang D, Zhang R, Liang Y, Pan W, Huang J and Dong D 2007 Vilsmeier–Haack Reactions of 2-Arylamino-3-acetyl-5,6-dihydro-4H-pyrans toward the Synthesis of Highly Substituted Pyridin-2(1H)-ones *J. Org. Chem.* **72** 8593
27. Bhat S S, Kumbhar A A, Heptullah H, Khan A A, Gobre V V, Gejji S P and Puranik V G 2011 Synthesis, electronic structure, DNA and protein binding, DNA cleavage, and anticancer activity of fluorophore-labeled copper(II) complexes *Inorg. Chem.* **50** 545
28. Ingle S A, Kate A N, Kumbhar A A, Khan A A, Rao S S and Gejji S P 2015 Synthesis and biological evaluation of copper(II) pyrenethiosemicarbazone *RSC Adv.* **5** 47476
29. Holland J P, Fisher V, Hickin J A and Peach J M 2010 Synthesis and Biological Evaluation of Copper(II) Pyrenethiosemicarbazone *Eur. J. Inorg. Chem.* **9** 48
30. Warren L E, Horner S M and Hatfield W E 1972 Chemistry of α -diketone-bis(thiosemicarbazone)copper(II) complexes *J. Am. Chem. Soc.* **94** 6392
31. Xie D, Kim S, Kohli V, Banerjee A, Yu M, Enriquez J S, et al. 2017 Hypoxia-Responsive ¹⁹F MRI Probes with Improved Redox Properties and Biocompatibility *Inorg. Chem.* **56** 6429
32. Raman N, Johnson R S and Sakthivel A 2007 Synthesis, spectral characterization of Schiff base transition metal complexes: DNA cleavage and antimicrobial activity studies *J. Chem. Sci.* **119** 303
33. Raman N and Johnson R S 2007 DNA cleavage, structural elucidation and anti-microbial studies of three novel mixed ligand Schiff base complexes of copper(II) *J. Serb. Chem. Soc.* **72** 983